Electronic structure, interfacial chemistry, and optical properties of $(\text{II-VI})_n/(\text{IV}_2)_m$ (110) superlattices

Liqiang Zhu
Department of Physics, Peking University, Beijing 100871, People's Republic of China

Enge Wang
Institute of Physics, Chinese Academy of Sciences, Beijing 100080, People's Republic of China

Liyuan Zhang
Department of Physics, Peking University, Beijing 100871, People's Republic of China

(Received 1 May 1997)

The detailed calculations of electronic structures of the $(\text{BeTe})_n/(\text{Si}_2)_m$, $(\text{BeTe})_n/(\text{Ge}_2)_m$, and $(\text{BeTe})_n/(\text{Si}_{1-x}\text{Ge}_{1+x})_m$ $[x\in(-1,+1)]$ (110) superlattices are performed by a semiempirical sp^3s^* tight-binding method with a wide range of $n,m\leq 20$. A strong quantum confinement effect is found that causes the states at the conduction- and the valence-band edges confined in two dimensions in the IV semiconductor wells. Results of how the band gap between the confined band-edge states and the lowest transition type change by varying the superlattice period are reported. Interfacial band structure and planar average of charge densities of states are presented for the BeTe-Si and BeTe-Ge boundaries. Two interface bands are identified in the upper region of the thermal gap in all the superlattices studied, which extend over a quite different region of **k** space. Furthermore, the calculated electronic structures of BeTe/SiGe (110) superlattice with a wide range of composition variations are found to be quite different from that of II-VI compound grown on pure IV semiconductors, but fairly close to their average. [S0163-1829(97)02939-1]

I. INTRODUCTION

Semiconductor superlattices consisting of alternate layers of different materials provide extra dimensions for tailoring material properties. The combination of controlled variations in the composition, strain, and thickness of the layers provides electronic and optical properties[1–3] unlike any ordinary bulk material that might lead to important applications in optoelectronics.[4–7] There has been great interest in the multilayer growth of II-VI compounds for optoelectronic device application in the visible-to-ultraviolet range as strong nonlinearities in these materials and their quantum wells have been recognized for many years.[8–10] Of particular note for the present work is the successful fabrication of II-VI/IV superlattices using molecular beam epitaxy, with each layer consisting of a few monolayers of the constituent materials.[11–13] Since a detailed picture of the electronic structure and stability will provide guidance for device applications, the systematic study of the II-VI/IV superlattice systems has become a necessity from a practical point of view.

In this paper, I examine theoretically the electronic structure of BeTe/Si, BeTe/Ge, and BeTe/SiGe superlattices by performing band structure calculation using the tight-binding method. Among the chalcogenides of Group II_A elements, BeTe is one of few which have the zinc-blende structure, a structure common to many well known II_B-VI and III-V semiconductors, and BeTe is also a potentially good semiconductors as revealed by many predecessors.[14,15] Nevertheless up to the present, to my knowledge, theoretical study of BeTe/Si, BeTe/Ge, and BeTe/SiGe superlattices has been neglected and there has been no report on the band structure of such systems, which is interesting both for the basic research and for practical applications. Besides the potential for industrial activities, the close lattice constants between BeTe and Si, Ge, or SiGe (Ref. 16) make the lattice mismatch smaller than 1.8, 1.5, and 0.2 %, respectively. An average lattice was used for each BeTe/IV superlattice, where IV is Si, Ge, or SiGe. The band edge shifts resulting from the small lattice mismatch are in the range of 0.01–0.05 eV,[17] which can be neglected within the tight-binding approximation.

In this study, I will present my calculations for the (110) growth direction. The (110) interface is nonpolar in a lattice-matched system, while the (100) and (111) interfaces are polar interfaces.[18] Therefore, the interface electric fields deduced from the differences in the nuclear charges of the two

TABLE I. Tight-binding parameters (in eV) for bulk BeTe. The off-site matrix elements ($\alpha,\beta=s,s^*,p,x$, and $y;i,j=a,c$) are written in the standard notations of Slater-Koster approximation.

$(s,p)_{ac}$	3.1376
$(s^*,p)_{ac}$	11.1116
$(s,p)_{ca}$	4.9266
$(s^*,p)_{ca}$	4.4876
(s,s)	−6.6814
(x,x)	0.4553
(x,y)	4.2536
$(s)_a$	−8.6164
$(s)_c$	1.8306
$(s^*)_a$	61.5396
$(s^*)_c$	22.9766
$(p)_a$	0.0109
$(p)_c$	4.2376

 © 1997 The American Physical Society

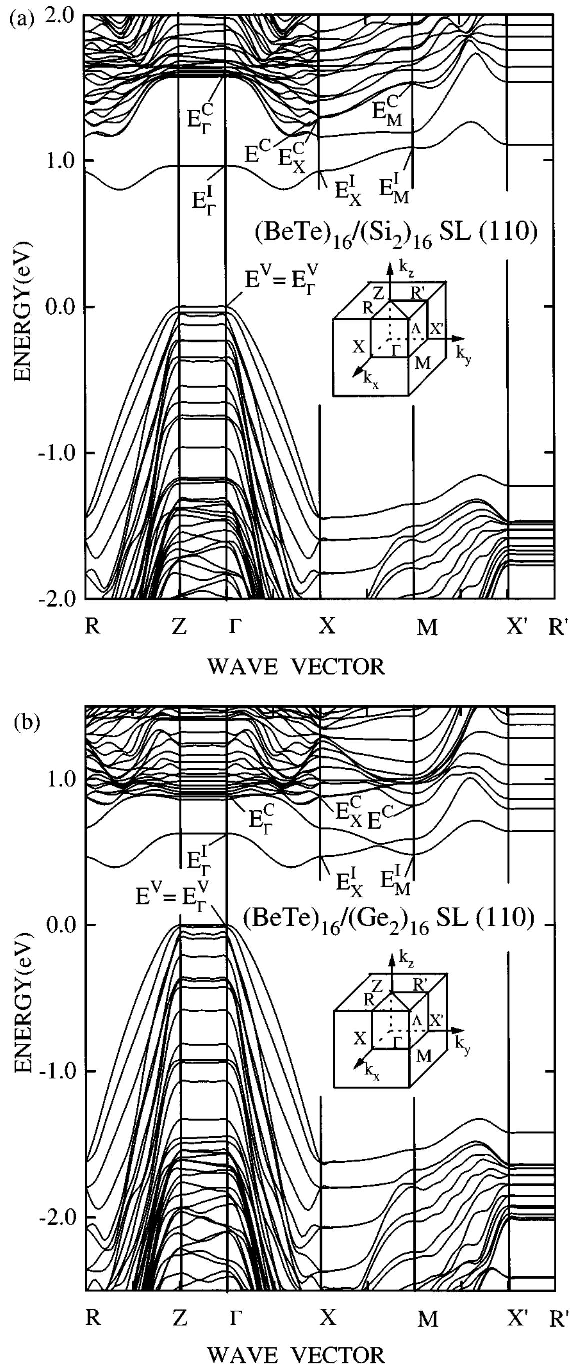

FIG. 1. Band structures of the $(BeTe)_{16}/(Si_2)_{16}$ and $(BeTe)_{16}/(Ge_2)_{16}$ (110) superlattices, (a) and (b), respectively, calculated by the first-neighbor sp^3s^* tight-binding method. The zero of energy corresponds to the top of the valence band of the superlattices. The inset shows the Brillouin zone of the $(BeTe)_{16}/(Si_2)_{16}$ and $(BeTe)_{16}/(Ge_2)_{16}$ (110) superlattices.

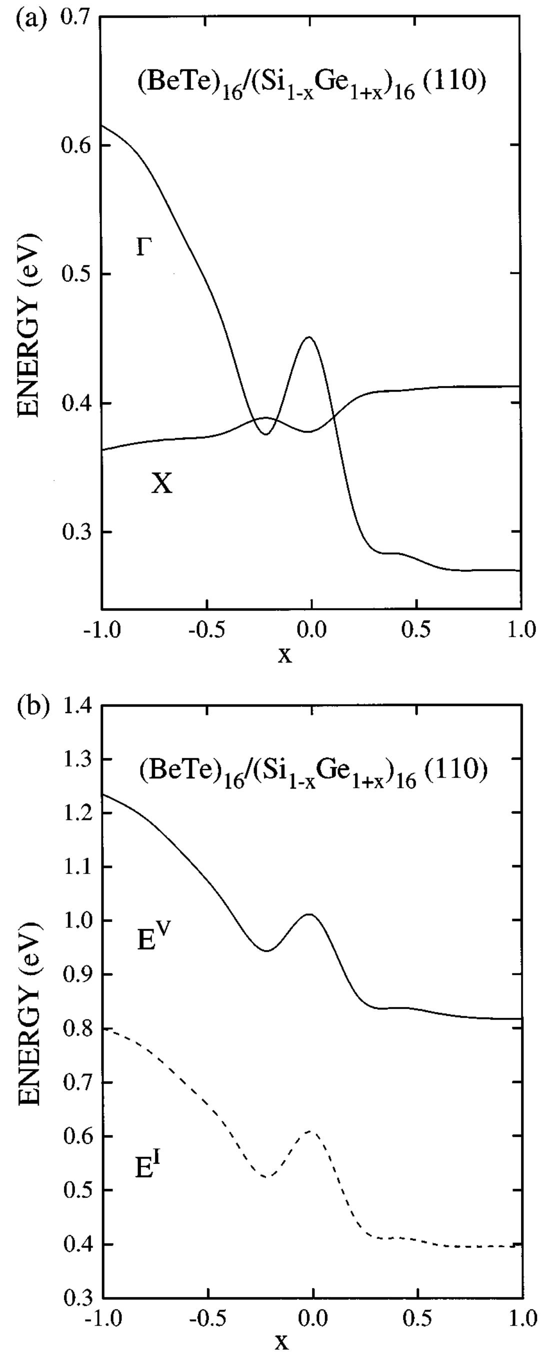

FIG. 2. (a) Difference of the interface states and the confined conduction band-edge states at some high symmetry points, where $\Gamma = \Gamma^C - \Gamma^I$ and $X = X^C - X^I$, (b) fundamental energy gap and interface state, in solid line and dashed line, respectively, for $(BeTe)_{16}/(Si_{1-x}Ge_{1+x})_{16}$ (110) superlattice with ideal interface. The zero of energy corresponds to the top of the valence band.

kinds of interface atoms in a (100) or (111) growth direction will disappear in the present (110) growth case. Some studies[19] have shown that, in a lattice-mismatched case, the atoms may no longer stay in planes perpendicular to the growth direction even for the (110) orientation. As a result this interface becomes slightly polar, which influences the band offset. However for the present nearly lattice-matched system, the out-of-plane motion is not included since the zero-field model[20] is well established. Further results of the charge densities of the confined states and interface states for these superlattice systems are also reported. A systematic study of the electronic and interfacial properties of II-VI/VI (110) superlattices with a wide range of epitaxial layer thickness has been carried out.

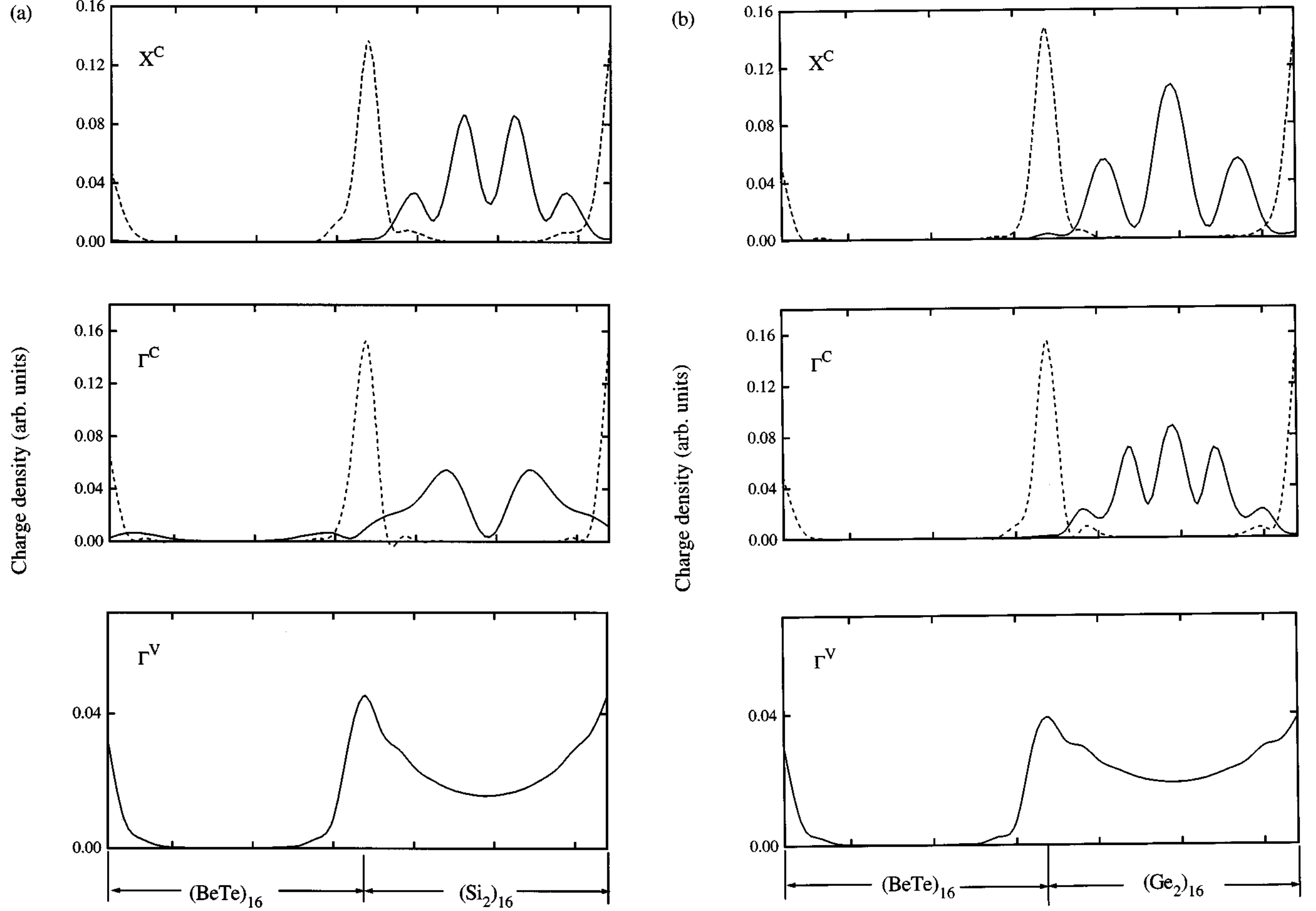

FIG. 3. Calculated planar average of the charge densities of the interface (dashed lines) and the confined band-edge (solid lines) states at Γ and X points for $(BeTe)_{16}/(Si_2)_{16}$ and $(BeTe)_{16}/(Ge_2)_{16}$ (110) superlattice, (a) and (b), respectively, with ideal interface.

II. TIGHT-BINDING TECHNIQUE

The tight-binding eigenstates of a superlattice can be expanded as a linear combination of atomic orbitals:[18,21]

$$|\mathbf{k},\lambda\rangle=\sum_{\xi,\alpha}\langle\xi,\mathbf{r}_\alpha,\mathbf{k}|\mathbf{k},\lambda\rangle|\xi,\mathbf{r}_\alpha,\mathbf{k}\rangle=\sum_{\xi,\alpha}C_{\xi\alpha}(\mathbf{k},\lambda)|\xi,\mathbf{r}_\alpha,\mathbf{k}\rangle, \tag{1}$$

where λ denotes the band index, ξ is a quantum number that runs over the basis orbitals s,s^*,p_x,p_y, and p_z on the different types of sites α in a unit cell. The N wave vectors $\mathbf{k}$ lie in the first Brillouin zone with the origin of the lth unit cell at $\mathbf{R}_l$, and $\mathbf{r}_\alpha$ represents the positions of the atoms in this unit cell. $C_{\xi\alpha}(\mathbf{k},\lambda)$ is the eigenwave function, which can be obtained by solving the Schrödinger equation

$$\sum_{\xi',\alpha'}[\langle\xi,\mathbf{r}_\alpha,\mathbf{k}|\mathbf{H}|\xi',\mathbf{r}_{\alpha'},\mathbf{k}\rangle-E_\lambda(\mathbf{k})\delta_{\xi\xi'}\delta_{\alpha\alpha'}]\langle\xi,\mathbf{r}_\alpha,\mathbf{k}|\mathbf{k},\lambda\rangle=0. \tag{2}$$

In this paper, only the nearest-neighbor interactions are included. The intramaterial elements in the tight-binding Hamiltonian can be uniquely formed by using the corresponding bulk parameters. While for the intermaterial elements at ideal interface, a simple average of the bulk parameters has been used. These bulk parameters are determined by fitting the first-principles calculations and experimental results. Yamaguchi's formulas[22] have been adapted to yield a self-consistent result at X-point energies. These parameters are tested against some well established bulk results.[14,15] For reference, I give the parameters used in my calculations for bulk BeTe in Table I. My parameters give the correct indirect gap of 2.95 eV and a correct order of conduction-band minima Γ-L-X for bulk BeTe. For bulk material Si I used the parameters given by Vogl *et al.*[23]

III. RESULTS AND DISCUSSION

A. Band structures

The band structures of the $(BeTe)_{16}/(Si_2)_{16}$ and $(BeTe)_{16}/(Ge_2)_{16}$ (110) superlattices are displayed in Fig. 1, where the zero of energy corresponds to the top of the valence band at $\mathbf{k}=0$. the inset shows the Brillouin zone of the $(BeTe)_{16}/(Si_2)_{16}$ and $(BeTe)_{16}/(Ge_2)_{16}$ (110) superlattices. Since the valence-band discontinuity of BeTe/Si and BeTe/Ge heterojunctions has not been established experimentally, here I assume their valence-band offset ΔE_v to be 1.03 eV (BeTe/Si) and 1.31 eV (BeTe/Ge) given by Harrison theory.[17] The irreducible part is indicated with the labels of the eight symmetry points (R,Z,Γ,X,M,X',R', and Λ), shown in the inset of Fig. 1, where the axis from the Γ point

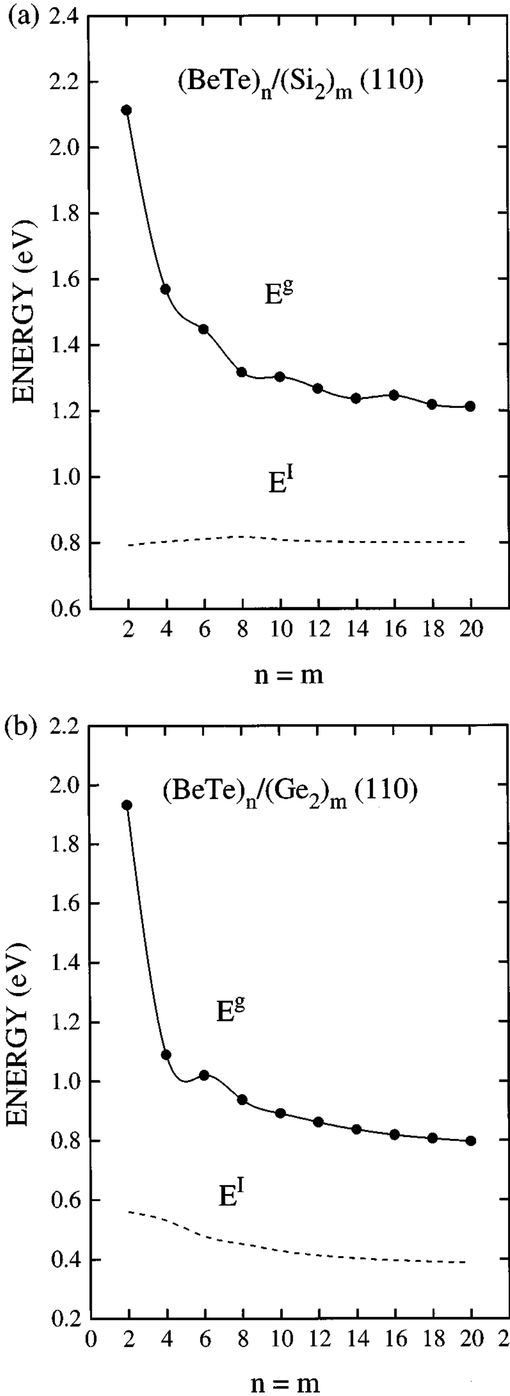

FIG. 4. Band gap E_g of $(\mathrm{BeTe})_n/(\mathrm{Si}_2)_m$ and $(\mathrm{BeTe})_n/(\mathrm{Ge}_2)_m$ (110) superlattices, (a) and (b), respectively, as a function of the number of layers $n=m$. The relative positions of the interface band E^I point are also drawn. The zero of the energy is the valence band maximum of the superlattice.

to the X point is normal to the projection of the Be-Si and Te-Si bonds on the (110) plane.

In Fig. 1, the top of the valence band is shown by E^V, which is located at the Γ point. The bottom of the conduction band is shown by E^C located at $\widetilde{X}$, which is near the X point, for $(\mathrm{BeTe})_{16}/(\mathrm{Si}_2)_{16}$ (110) superlattice and at M for $(\mathrm{BeTe})_{16}/(\mathrm{Ge}_2)_{16}$ (110) superlattice. The other lowest conduction band states are E_Γ^C, E_X^C, and E_M^C, at the Γ, X, and M points, respectively.

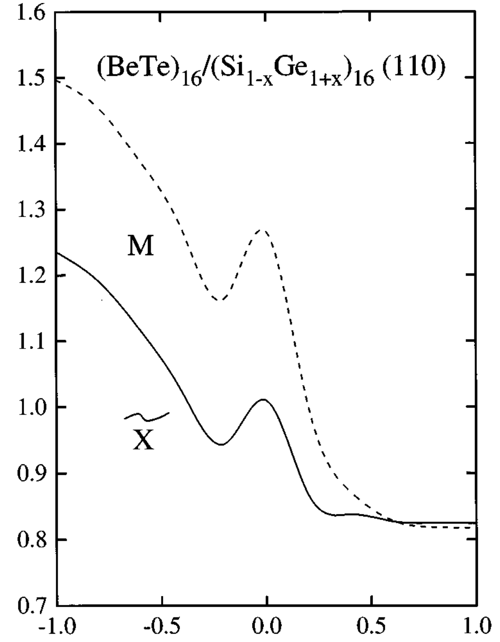

FIG. 5. Energy minima at some high symmetry points at $\widetilde{X}$ point (solid line) and M point (dashed line) for $(\mathrm{BeTe})_{16}/(\mathrm{Si}_{1-x}\mathrm{Ge}_{1+x})_{16}$ (110) superlattice with ideal interface. The lowest transition is the Γ-to-M ($x>0.615$) and Γ-to-$\widetilde{X}$ ($x<0.615$). The zero of energy corresponds to the top of the valence band of the superlattices.

Two interface state bands, lying in the upper region of the thermal gap, are found to be clearly localized at the identical interfaces of the BeTe/Si and BeTe/Ge superlattices, where the Be-Si and Te-Si bonds are equally present in the BeTe/Si system as are Be-Ge and Te-Ge bonds in the BeTe/Ge system. It is found that the interface states appear over an extended region of **k** space.

In the $(\mathrm{BeTe})_n/(\mathrm{Si}_{1-x}\mathrm{Ge}_{1+x})_m$ superlattices, a continuous range of materials parameters, tunable by changing the composition x, is allowed because of the presence of a pseudobinary semiconductor SiGe alloy. The tight-binding parameters for bulk material $\mathrm{Si}_{1-x}\mathrm{Ge}_{1+x}$ alloy can be written as

$$E(A_{1-x}B_{1+x})=[(1-x)E(A)+(1+x)E(B)]/2. \quad (3)$$

The difference of positions between the interface state and the confined conduction band-edge state at some high symmetry points by continuously changing the composition x, where $\Gamma = \Gamma^C-\Gamma^I$ and $X=X^C-X^I$, has been analyzed in Fig. 2(a). The fundamental energy gap versus composition x is given in Fig. 2(b) in solid line, the interface state is also drawn in the figure in dashed line, where the zero of energy corresponds to the top of valence band. For a fixed superlattice period $n=m=16$, the interface state energy at $\widetilde{X}$ point and the energy gap reach a maximum concurrently as $x=0$. The tendencies of energy gap and interface state position are quite similar by varying the composition x.

B. Confined states and localized states

The large-band-gap BeTe layers cause quantum confinement in the small gap Si or Ge quantum wells. A detailed description of the planar averages of the charge densities of

the Γ and X band-edge states is shown in Figs. 3(a) and 3(b) for $(BeTe)_{16}/(Si_2)_{16}$ and $(BeTe)_{16}/(Ge_2)_{16}$ (110) superlattices, respectively, with ideal interface in solid lines. The interface states at Γ and X are also analyzed in Fig. 3, drawn in dashed lines. From Fig. 3, one can see that all the band-edge states are confined in two dimensions—silicon or germanium wells. Therefore, it is reasonable to believe that the crowded subbands in Fig. 1, consisting of the valence and conduction bands of the superlattice, originate from those of IV semiconductors by the zone folding effects.

In order to check how the interface states are affected by the choice of valence-band offset ΔE_v, I study the interfacial properties of $(BeTe)_{16}/(Si_2)_{16}$ and $(BeTe)_{16}/(Ge_2)_{16}$ (110) superlattices by varying ΔE_v. It shows that in all the superlattice systems examined, the relative positions of the interface states are changed by varying ΔE_v, but they do not disappear from the gap for all possible valence-band offsets. It is found in the superlattices studied parts of the interface band with higher energy are pushed into the conduction valence band region, in agreement with the experimental consensus.[24]

C. Energy gap

The fundamental band gaps of the $(BeTe)_n/(Si_2)_m$ and $(BeTe)_n/(Ge_2)_m$ (110) superlattices with ideal interfaces are given as a function of $n=m$ in Figs. 4(a) and 4(b), respectively. The interface states E^I are plotted, dashed lines in Fig. 4, for both systems, where the zero of energy corresponds to the top of the valence band. It is found the lowest transition is the indirect Γ-to-$\tilde{X}$ for all BeTe/Si superlattices, where $\tilde{X}$ is near the X point. For the BeTe/Ge system, it is Γ-to-M ($n=m>10$) and Γ-to-$\tilde{X}$ ($n=m\leqslant 10$).

The quantum confinement is most dramatic, as illuminated in Fig. 4, as the band gap rises sharply by decreasing the superlattice period. However, it is found that the fundamental band gap of the $(BeTe)_n/(Si_2)_m$ or $(BeTe)_n/(Ge_2)_m$ (110) superlattices does not change significantly, as expected, by varying the BeTe layer thickness at a fixed number of Si or Ge layers. It is concluded that the Si or Ge layer thickness is crucial in determining the fundamental gap of the BeTe/Si or BeTe/Ge superlattice.

Furthermore, Fig. 5 shows how the relative positions of the two minima of the valence band at $\tilde{X}$ point (solid line) and the M point (dashed line) change by varying the composition x, where the zero of energy corresponds to the top of valence band. One can see the lowest transition type undergoes a change between Γ-to-M and Γ-to-$\tilde{X}$ at $x=0.615$.

IV. CONCLUSION

A systematic investigation of electronic structure, interfacial chemistry and optical transition in $(II\text{-}VI)_n/(IV_2)_m$ (110) superlattices has been performed for a wide range of $n,m\leqslant 20$ by using a semiempirical tight-binding method. Two empty interface bands are identified in the upper region of the gap in the superlattice, which extend over a quite different region of **k** space. It is found the SiGe layer plays a dominant role in determining the fundamental gap of the superlattice system due to the strong quantum confinement effect. For a valence-band discontinuity $\Delta E_v=1.03$ eV for BeTe/Si superlattice and $\Delta E_v=1.31$ eV for BeTe/Ge superlattice, given by the Harrison theory, the band gap between the confined band-edge states increases sharply (up to 2.11 eV for BeTe/Si and 1.93 eV for BeTe/Ge at the $\tilde{X}$ point for $n=m=2$) by decreasing the superlattice period. By checking the electronic structure of $(BeTe)_n/(Si_{1-x}Ge_{1+x})_m$ with the composition $x\in(-1,+1)$ for a wide range of $n,m\leqslant 20$, the electronic and interfacial properties are found to be quite different from that of those II-VI compounds grown on pure IV semiconductors, but fairly close to their average in all cases. It is concluded that behavior of the interface states of these calculated systems has no major difference within the composition x range examined. These results presented in this work should establish the understanding of the fundamental electronic properties of the superlattices fabricated from II-VI and IV semiconductors.

ACKNOWLEDGMENTS

This work was partly supported by Chinese NSF Grant No. 69525409.

[1] J. L. Pérez-Díaz and M. C. Muñoz, Phys. Rev. Lett. **76**, 4967 (1996).

[2] M. S. Salib, H. A. Nickel, G. S. Herold, A. Petrou, B. D. McCombe, R. Chen, K. K. Bajaj, and W. Schaff, Phys. Rev. Lett. **77**, 1135 (1996).

[3] A. Messica, A. Soibel, U. Meirav, A. Stern, H. Shtrikman, V. Umansky, and D. Mahalu, Phys. Rev. Lett. **78**, 705 (1997).

[4] G. C. Osbourn, J. Appl. Phys. **53**, 1586 (1982).

[5] T. P. Pearsall, F. H. Pollak, J. C. Bean, and R. Hull, Phys. Rev. B **33**, 6821 (1986).

[6] J. C. Bean, Science **230**, 127 (1985).

[7] T. P. Pearsall, F. Bevk, L. C. Feldman, J. M. Bonar, J. P. Mannaerts, and A. Ourmazd, Phys. Rev. Lett. **58**, 729 (1987).

[8] R. C. Miller, D. A. Kleinman, and A. Savage, Phys. Rev. Lett. **11**, 146 (1963).

[9] F. W. Scholl and C. L. Tang, Phys. Rev. B **8**, 4607 (1973).

[10] A. J. Fischer, D. S. Kim, J. Hays, W. Shan, J. J. Song, D. B. Eason, J. Ren, J. F. Schetzina, H. Luo, J. K. Furdyna, Z. Q. Zhu, T. Yao, J. F. Klem, and W. Shafer, Phys. Rev. Lett. **73**, 2368 (1994).

[11] L. T. Romano, R. D. Bringans, J. Knall, D. K. Biegelsen, A. Garcia, J. E. Northrup, and M. A. O'Keefe, Phys. Rev. B **50**, 4416 (1994).

[12] X. C. Zhou and W. P. Kirk, Mater. Res. Soc. Symp. Proc. **318**, 307 (1994).

[13] X. C. Zhou, G. F. Spencer, F. Li, and W. P. Kirk, AIP Conf. Proc. **325**, 227 (1995).

[14] D. J. Stukel, Phys. Rev. B **2**, 1852 (1970).

[15] R. L. Sarkar and S. Chtterjee, J. Phys. C **10**, 47 (1977).

[16] J. C. Phillips, *Bonds and Bands in Semiconductors* (Academic, New York, 1973), p. 169.
[17] W. A. Harrison, *Electronic Structure and the Properties of Solids* (Freeman, San Francisco, CA, 1980).
[18] E. G. Wang and C. S. Ting, Phys. Rev. B **51**, 9791 (1995).
[19] N. E. Christensen and I. Gorczyca, Phys. Rev. B **44**, 1707 (1991).
[20] T. Saito and T. Ikoma, Phys. Rev. B **45**, 1762 (1992); J. Pollmann and S. T. Pantelides, *ibid.* **21**, 709 (1980); J. Shen, J. D. Dow, and S. Y. Ren, J. Appl. Phys. **67**, 376 (1990).
[21] E. G. Wang, C. F. Chen, and C. S. Ting, J. Appl. Phys. **78**, 1832 (1995).
[22] E. Yamaguchi, J. Phys. Soc. Jpn. **57**, 2461 (1988).
[23] P. Vogl, H. P. Hjalmarson, and J. D. Dow, J. Phys. Chem. Solids **44**, 365 (1983).
[24] A. G. Milnes and D. L. Feucht, *Heterojunctions and Metal-Semiconductor Junctions* (Academic, New York, 1972).